Fluoride ion donor properties of group 13 trifluorides (MF_3, M = Al, Ga, In, Tl) and crystal structures of $InF_3 \cdot 3SbF_5$, $TlF_3 \cdot 3SbF_5$ and $TlF_3 \cdot AsF_5 \cdot 2HF$†

Zoran Mazej* and Evgeny Goreshnik

Received (in Victoria, Australia) 2nd July 2010, Accepted 20th August 2010
DOI: 10.1039/c0nj00514b

Reactions between strong Lewis acids (*i.e.* AsF_5, SbF_5) and MF_3 (M = Al, Ga, In, Tl) in anhydrous hydrogen fluoride at ambient temperature proceeded only in three cases, yielding $InF_3 \cdot 3SbF_5$, $TlF_3 \cdot 3SbF_5$, $TlF_3 \cdot AsF_5 \cdot 2HF$ and $TlF_3 \cdot AsF_5$. Crystal structure of $InF_3 \cdot 3SbF_5$ consists from infinite chains of In atoms connected by three SbF_6 units, with two bridging fluorine atoms (F_b) in *cis*-position. Due to the strong interaction of SbF_6 units with In^{3+}, the Sb–F_b bonds are significantly elongated (200.7(4) pm). Such long Sb–F_b bonds have been observed in the crystal structure of SbF_5. The crystal structure of $TlF_3 \cdot 3SbF_5$ is built from slabs where thallium atoms are connected by SbF_6 units. The thallium is nine-fold coordinated by fluorine atoms in the shape of a tricapped trigonal prism. In the crystal structure of $TlF_3 \cdot AsF_5 \cdot 2HF$ there are puckered layers, composed of rectangular rings made of Tl and F atoms. The seven-fold coordination around each Tl is completed by three axial fluorine atoms, provided by one HF molecule and two AsF_6 units arranged below and above the puckered layers forming infinite slabs on that way. The second molecule of HF is placed between the slabs. Vibrational spectra of isolated $InF_3 \cdot 3SbF_5$, $TlF_3 \cdot 3SbF_5$, and $TlF_3 \cdot AsF_5$ are consistent with the presence of highly deformed SbF_6/AsF_6 octahedra.

Introduction

According to Brønsted and Lowry definition, an acid is a proton donor and a base is a proton acceptor. An acid–base reaction always involves a transfer of proton allowing a quantitative comparison of different Brønsted acids. Estimating the strength of Lewis acids represents a problem, since no such common relationship exists. Various approaches have been used for a qualitative description of strengths of Lewis acids.[1] A quantitative scale (pF^- scale) for Lewis acidity based on fluoride ion affinities of free gaseous molecules was reported first time in 2001.[2] Fluoride ion has a small size and high basicity and because of that it reacts essentially with all Lewis acids. Therefore the fluoride ion affinity (or enthalpy of reaction between Lewis acid and fluoride ion) could serve as a quantitative scale of Lewis acids.[1]

Group 13 trifluorides (MF_3, M = Al, Ga, In) are according to the pF^- scale very strong Lewis acids placed between SbF_5 and AsF_5. The SbF_5 has been for a long time considered as the strongest Lewis acid. Recent high level electronic calculations[3] confirmed previous experimental results (*i.e.* $[AsF_4]^+[PtF_6]^-$ is known,[4] meanwhile analogue compound with between AsF_5 and SbF_5 is not) that MF_5 (M = Os, Ir, Pt, Au) are even stronger than SbF_5. Actual pF^- values for solid MF_3 are certainly lower because in the case of polymeric solids pF^- values have to be corrected for association energies resulting in smaller pF^- values than for free molecules.[2]

In the present work the results of reactions between MF_3 (M = Al, Ga, In, Tl) and Lewis acids (AsF_5, SbF_5) in anhydrous hydrogen fluoride (aHF) are described.

Results and discussion

Synthesis

InF_3 and TlF_3 completely dissolved in anhydrous hydrogen fluoride (aHF), acidified with large excess of SbF_5, yielding colourless solutions from which colourless $MF_3 \cdot 3SbF_5$ (M = In, Tl) were isolated (eqn (1)). The analogous reactions with AlF_3 and GaF_3 did not proceed:

$$MF_3 + 3SbF_5 \xrightarrow[298\ K]{HF} MF_3 \cdot 3SbF_5\ (M = In, Tl) \quad (1)$$

InF_3 dissolves in aHF, only when aHF is acidified with large excess of SbF_5, *i.e.* when molar ratio $n(InF_3) : n(SbF_5)$ is much higher than 1 : 3. This could be explained by the fact that acidity of fluorine-bridged Sb_nF_{5n} (n = 1, 2, 3, 4) and of n monomeric SbF_5 molecules increases with increasing n (*i.e.* fluoride ion affinities of $SbF_{5(g)}$ = 503–515 kJ mol^{-1}), $Sb_2F_{10(g)}$ 556–559 kJ mol^{-1}, $Sb_3F_{15(g)}$ = 572 kJ mol^{-1}, $Sb_4F_{20(g)}$ = 580 kJ mol^{-1}, $2SbF_{5(g)}$ = 667–671 kJ mol^{-1}, $3SbF_{5(g)}$ = 728–767 kJ mol^{-1}, and $4SbF_{5(g)}$ = 855 kJ mol^{-1}).[5]

The lack of observed reactions in the case of Al and Ga could be also due to kinetic inertness. For example, it is well known that α-AlF_3 is nonreactive with little or no catalytic

Jožef Stefan Institute, Jamova 39, SI-1000 Ljubljana, Slovenia. E-mail: zoran.mazej@ijs.si; Fax: (+386) 1 477 3155; Tel: (+386) 1 477 3301

† Electronic supplementary information (ESI) available: X-ray powder diffraction pattern of $TlF_3 \cdot AsF_5$ (Table S1), Infrared spectra of ground crystals of $TlF_3 \cdot AsF_5 \cdot 2HF$ (Fig. S1 and S2) and vibrational spectra of $TlF_3 \cdot AsF_5$ (Fig. S3). CSD reference numbers 783217–783219. For ESI and crystallographic data in CIF or other electronic format see DOI: 10.1039/c0nj00514b

activity, meanwhile β- and other forms (η-, θ-, κ-) of AlF_3 are more reactive.[6,7] The highest reactivity is observed for X-ray amorphous so called high surface *HS*-AlF_3 which does not have a regular bulk structure.[8,9] Alfa phase has a closed-packed structure, whereas beta and other phases, structurally related to β-AlF_3, have more open structures. Because of that, reaction between $KAlF_4$ and excess of SbF_5 in aHF has been also tried (eqn (2)). An attempt was made to prepare $AlF_3{\cdot}nSbF_5$ from $KAlF_4$ *in situ* by displacement of a weaker Lewis acid (AlF_3) with a stronger one (SbF_5).

$$KAlF_3 + (n+2)SbF_5 \xrightarrow[298\,K]{HF} KSb_2F_{11} + AlF_3 \cdot nSbF_5 \quad (2)$$

Instead of the desired $AlF_3{\cdot}nSbF_5$ phase only AlF_3 was observed with by-product KSb_2F_{11}.

Reaction with AsF_5 in aHF proceeded only in the case of TlF_3. First unstable $TlF_3{\cdot}AsF_5{\cdot}2HF$ is formed which further decomposes during the pumping on a high vacuum to $TlF_3{\cdot}AsF_5$ (eqn (3)).

$$TlF_3 + AsF_5 \xrightarrow[298\,K]{HF} TlF_3 \cdot AsF_5 \cdot 2HF \xrightarrow[-2HF]{pumping} TlF_3 \cdot AsF_5 \quad (3)$$

From a purely thermodynamic standpoint, the fluoride ion affinity is only one of the factors that will determine if reaction would proceed or not. Neglecting the entropy, difference between lattice energies of reactants and products is another governing factor. Unsuccessful attempts to synthesize $MF_3{\cdot}nSbF_5$ (M = Al, Ga) could be ascribed to their higher lattice energies of AlF_3 and GaF_3 in comparison to InF_3 and TlF_3.[10,11] For the latter, fluoride ion affinity of Sb_nF_{5n} ($n \geq 1$) and lattice energies of $InF_3{\cdot}3SbF_5$ and $TlF_3{\cdot}3SbF_5$ are enough to overcome the lattice energies of starting trifluorides and make reaction between InF_3/TlF_3 and SbF_5 thermodynamically favourable.

Crystal structures

Crystal structure of $InF_3{\cdot}3SbF_5$. Crystal structure of $InF_3{\cdot}3SbF_5$ consists of infinite chains (Fig. 1) of indium atoms connected by three SbF_6 units, with two bridging fluorine atoms (F_b, *i.e.* F2) in *cis*-position (Fig. 2). In1 atom occupies the 2*b* Wyckoff position with $\bar{3}$ symmetry, and the Sb1 atom is located at a site with twofold symmetry (Wyckoff 6*f*). Very

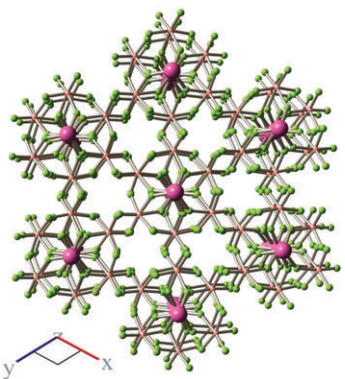

Fig. 1 Packing of infinite –[In–(F–SbF_4–F)$_3$–In]– chains in the crystal structure of $InF_3{\cdot}3SbF_5$.

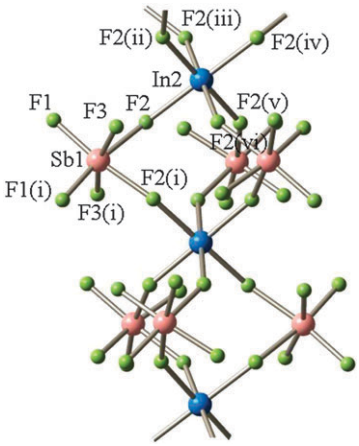

Fig. 2 Part of the infinite chain in the crystal structure of $InF_3{\cdot}3SbF_5$. Symmetry operations used for generation of equivalent atoms: (i) $x-y, -y, 0.5-z$ (ii) $x-y, -1+x, -z$ (iii) $1+y, 1-x+y, -z$ (iv) $2-x, -y, -z$ (v) $2-x+y, 1-x, z$ (vi) $1-y, -1+x-y, z$.

long Sb–F_b(–In) bond distance (200.7(4) pm) is comparable with the Sb–F_b bond lengths [198(5)–206(5) pm] found in the crystal structure of solid SbF_5,[4] where SbF_5 units are connected in tetrameric rings [$(SbF_5)_4$] by *cis*-fluorine atoms. Although, there are numerous examples of fluorine bridged adducts, in neither of them such elongation of Sb–F_b bond has been observed, *i.e.* Sb–F_b = 196.4(3) pm ($[Au(HF)_2](SbF_6)_2{\cdot}HF$),[12] 195.15(5) pm ($CrF_5{\cdot}SbF_5$),[13] 195.4(16) and 199.0(14) pm ($UF_5{\cdot}2SbF_5$),[14] 194.2(6) pm ($MoF_4O{\cdot}SbF_5$),[15] 192.7(4) pm ($TcO_2F_3{\cdot}SbF_5$),[16] 194.5(4) pm ($ReO_2F_3{\cdot}SbF_5$).[16] Much longer Sb–F_b bond length has been theoretically predicted (210.38 pm) only in so far unknown dinuclear anion $[F_5Au\cdots F\cdots SbF_5]^-$.[17] what is in agreement with higher Lewis acidity of AuF_5 in comparison to SbF_5.

Bond lengths between Sb and terminal fluorine atoms (F_t) in the crystal structure of $InF_3{\cdot}3SbF_5$ are in the range 183.9(4)–184.9(4) pm and are close to Sb–F_t distances in solid SbF_5 (177(5)–187(5) pm).[4] Fluorine atoms around indium metal form quite regular octahedra with bond lengths In–F = 207.5(4) pm similar as to that in InF_3 (205.3(3) pm).[5] The F–In–F bond angles in InF_6 octahedra are 87.67(16) and 92.33(16)°, respectively. Although the bridging fluorine atoms are closer to antimony than to indium atoms, the SbF_6 octahedra are strongly deformed (F–Sb–F bond angles are in the range from 81.5(2) to 99.5(3)°). Therefore a description $InF_3{\cdot}3SbF_5$ is more preferable than $In(SbF_6)_3$.

Crystal structure of $TlF_3{\cdot}3SbF_5$. The crystal structure of $TlF_3{\cdot}3SbF_5$ consists of slabs (Fig. 3) where thallium atoms are connected by SbF_6 units (Fig. 4). Tl1 atom is at a 2*d* site with three-fold symmetry.

Each SbF_6 unit bridges to two thallium atoms, with three bridging fluorine atoms in *facial* position (Fig. 5). As expected, Sb–F_b bond lengths (Sb–F_b = 189.4(6) pm, 197.0(6) pm, and 197.7(6) pm) are longer than Sb–F_t ones (183.1(6) pm, 183.3(6) pm, 183.4(6) pm). Although the Sb–F_b bond lengths are shorter than Sb–F_b distances in $InF_3{\cdot}3SbF_5$, the longest two bonds are still significantly longer then Sb–F_b bonds observed in other fluorine bridged adducts. This indicates that TlF_3 is

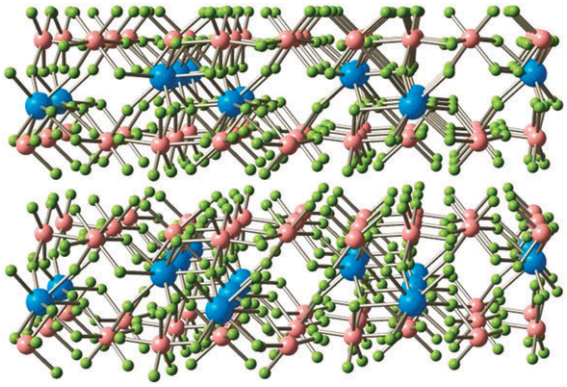

Fig. 3 View along *a*-axis showing the packing of slabs in the crystal structure of $TlF_3{\cdot}3SbF_5$.

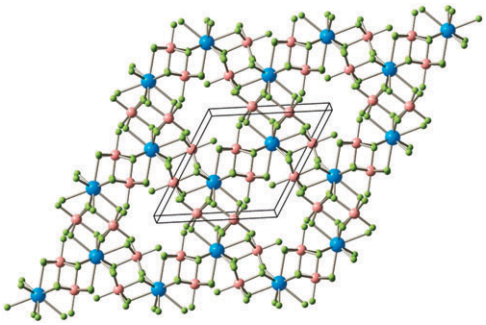

Fig. 4 View along *c*-axis (perpendicular on the slab) in the crystal structure of $TlF_3{\cdot}3SbF_5$.

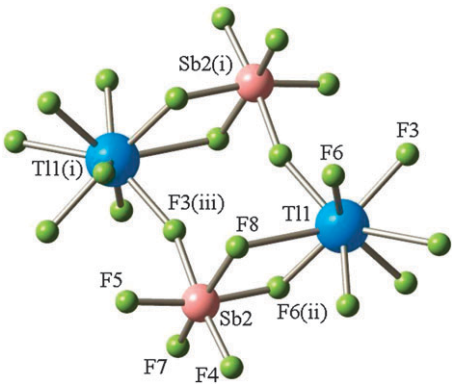

Fig. 5 SbF_6 units, with three bridging fluorine atoms in *facial* position, connecting two Tl atoms in the crystal structure of $TlF_3{\cdot}3SbF_5$. Symmetry operations used for generation of equivalent atoms: (i) $1 - x, 1 - y, 1 - z$ (ii) $1 - y, x - y, z$ (iii) $y, 1 - x + y, 1 - z$.

also a poor fluoride ion donor, although much better than InF_3. Although the elongation of Sb–F_b bonds in $TlF_3{\cdot}3SbF_5$ is not so pronounced as in $InF_3{\cdot}3SbF_5$, the former formulation is still more appropriate than ionic one, *i.e.* $Tl(SbF_6)_3$.

The polyhedron around the metal center is basically a tricapped trigonal prism (Fig. 6a), whose triangular faces are formed by fluorine ligands provided by six SbF_6 units. All rectangular faces of the prism are capped by fluorine ligands. This way coordination number nine is achieved for the Tl atom. One triangular face of trigonal prism is staggered by $\sim 5^\circ$ with respect to the other one (Fig. 6b).

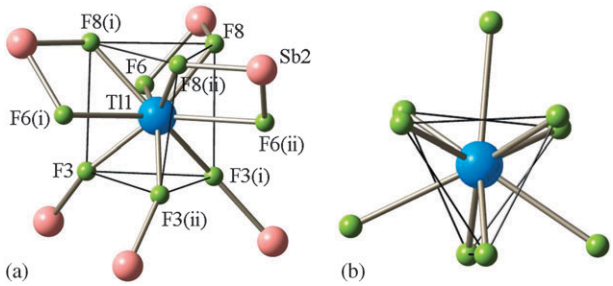

Fig. 6 Nine-fold coordination of Tl atom in the shape of a tricapped trigonal prism (a) and one triangular face of trigonal prism is staggered against the other one (b) in $TlF_3{\cdot}3SbF_5$. Symmetry operations used for generation of equivalent atoms: (i) $1 - x + y, 1 - x, z$ (ii) $1 - y, x - y, z$.

The Tl–F3 and Tl–F8 bond lengths are significantly shorter (218.4(6) and 220.5(6) pm, respectively) than Tl–F6 distances (259.3(8) pm), however, this difference is balanced by respective distances to the Sb atoms as Sb–(F3/F8) (197.7(6)/197.0(6) pm) are considerably longer than Sb–F6 (189.4(6) pm). For comparison, in TlF_3 (where Tl is 8-fold coordinated), Tl–F distances are 1×209 pm; 2×220 pm, 2×223 pm, 1×224 pm and 2×249 pm.[18]

Crystal structure of $TlF_3{\cdot}AsF_5{\cdot}2HF$. In the crystal structure of $TlF_3{\cdot}AsF_5{\cdot}2HF$, thallium atoms are connected *via* fluoride anions, resulting in the formation of puckered layers, composed of rectangular rings (Fig. 7).

The seven-fold coordination around each Tl is completed by three axial fluorine atoms, provided by HF molecule and two AsF_6 units arranged below and above the puckered layers (Fig. 8). In this way infinite slabs are formed which are connected *via* hydrogen bonds only. There are "free" molecules of HF placed between the slabs. Another example of a compound with coordinated and non-coordinated HF molecules is $Au(SbF_6)_2{\cdot}4HF$.[12]

In each AsF_6 unit there are four short [As–F5: 167.9(8), As–F4: 168.3(7), As–F3: 170.8(7), As–F2: 170.9(8) pm] and two long As–F bonds [As–F1: 178.0(7) pm, As–F6: 178.8(7) pm]. The latter are bridging ones and connect AsF_6 units to Tl atoms (Fig. 9). Both sets of bond distances are in the range of previously reported bond lengths between As and terminal or bridging fluorine atoms, respectively.[19]

There are three ideal geometries known for coordination number seven: monocapped octahedron, monocapped trigonal prism in which a seventh ligand has been added to a rectangular face and a pentagonal bipyramid. The coordination of fluorine

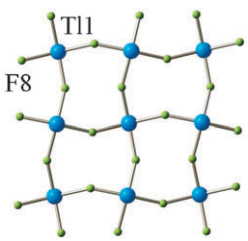

Fig. 7 Part of the puckered layer in the crystal structure of $TlF_3{\cdot}AsF_5{\cdot}2HF$ showing rectangular rings (HF molecules and AsF_6 units are omitted for clarity).

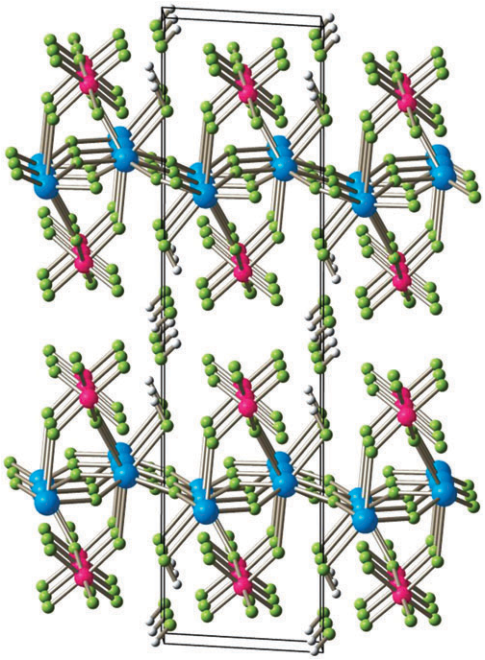

Fig. 8 Fragment of the crystal structure of $TlF_3{\cdot}AsF_5{\cdot}2HF$ showing the packing of slabs.

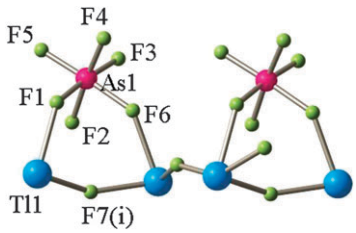

Fig. 9 Part of the crystal structure of $TlF_3{\cdot}AsF_5{\cdot}2HF$ showing the connectivity of Tl atoms and AsF_6 units with bridging fluorine atoms in *cis* positions. Symmetry operations used for generation of equivalent atoms: (i) $1 - x$, $0.5 + y$, $1.5 - z$.

atoms around Tl in $TlF_3{\cdot}AsF_5{\cdot}2HF$ is irregular (C.N. = 7) and it could be hardly described with idealized structures (Fig. 10).

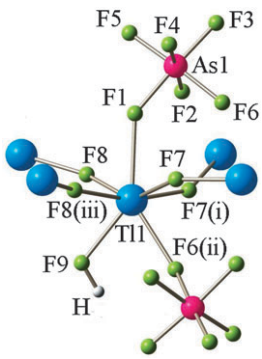

Fig. 10 Part of the crystal structure of $TlF_3{\cdot}AsF_5{\cdot}2HF$, showing the coordination around Tl atom. Symmetry operations used for generation of equivalent atoms: (i) $1 - x$, $0.5 + y$, $1.5 - z$ (ii) $1 - x$, $-0.5 + y$, $1.5 - z$ (iii) $2 - x$, $-0.5 + y$, $1.5 - z$.

The Tl–F(–Tl) bond lengths ($Tl1–F7^{i}$ = 207.0(6), $Tl1–F8^{iii}$ = 207.5(6), Tl1–F8 = 214.7(6) and Tl1–F7 = 216.5(6) pm) are significantly shorter than Tl–F(–AsF_5) [Tl1–F9 = 228.4(6), $Tl1–F6^{ii}$ = 230.7(7)] and Tl–F(–H) [Tl1–F1 = 241.6(7) pm] bond distances. In $KTlF_4$ where Tl is also coordinated by seven fluoride ligands, the Tl–F distances are in the range from 202 to 249 pm.[20]

It's well known that oxygen and fluorine atoms are sometimes technically difficult to distinguish by X-ray diffraction. In the crystal structure of $TlF_3{\cdot}AsF_5{\cdot}2HF$ the positions of hydrogen atoms could not be unambiguously determined. Therefore, grown crystals could hypothetically also have composition $TlF_3{\cdot}AsF_5{\cdot}2H_2O$, $TlF_3{\cdot}AsF_5{\cdot}2H_2O/HF$ or even $(H_3O)Tl(F)F_2(AsF_6)$, if we assume that non-coordinated HF is $[H_3O]^+$ cation and that, instead of Tl atom coordinated HF, we have only terminal fluorine atom. Both options are highly unlikely. The first option could be excluded because in AsF_5/aHF superacid systems water behaves as a very strong base and consequently displaces the weaker base HF from $[H_2F]^+$, thus forming $[H_3O]^+$ ions directly in solution.[21] The second option is also not very reliable because there would be a highly electronegative terminal fluorine atom in the neighbourhood of three protons belonging to $[H_3O]^+$ cation. The final proof for $TlF_3{\cdot}AsF_5{\cdot}2HF$ composition came from infrared spectra (see Fig. S1 and S2†) of ground crystals, where no vibrational bands were observed in 1000–4000 cm^{-1} region. In that region $[H_3O]^+$ salts give very sharp and moderately strong band at around 1600 cm^{-1} [$\delta_{as}(H_3O^+)$] and very broad double band in 3000–3500 cm^{-1} region [$\nu_{as}(H_3O^+)$ and $\nu_s(H_3O^+)$].[22] The vibrations belonging to molecules of water are found in the same ranges (bending and stretching vibrations at around 1600 and 3200–3500 cm^{-1}, respectively).[23]

Vibrational spectroscopy

Vibrational spectra of $InF_3{\cdot}3SbF_5$ and $TlF_3{\cdot}3SbF_5$ are shown in Fig. 11 and 12 and frequencies are given in Table 1 and 2.

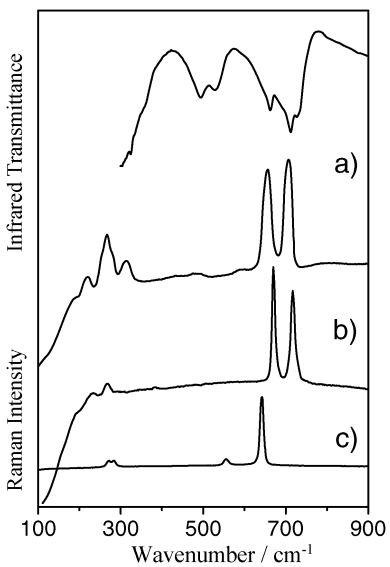

Fig. 11 Vibrational data of: (a) $InF_3{\cdot}3SbF_5$, (b) liquid SbF_5, (c) $InSbF_6$.[28]

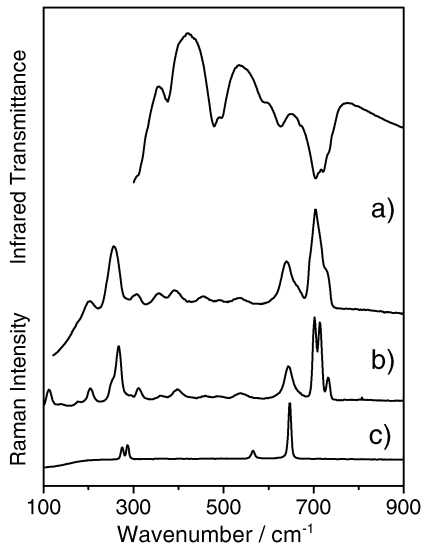

Fig. 12 Vibrational data of $TlF_3{\cdot}3SbF_5$ [(a) powder; (b) single crystal] and (c) $TlSbF_6$.

Table 1 Vibrational data of $InF_3{\cdot}3SbF_5$ and liquid SbF_5[25,27]

$InF_3{\cdot}3SbF_5$		SbF_5 (liquid)		Tentative Assignments[a]
IR[b]	*R*	IR	*R*	
730(s)		742(s)		ν(Sb–F_t)
	707(vs)		718(s)	ν(Sb–F_t)
713(vs)		705(s)		ν(Sb–F_t)
665(m)	657(s)	669(s)	670(s)	ν(Sb–F_t)
533(m)				ν(Sb–F_b–In)
496(m)		450(w,br)		ν(Sb–F_b–In)
			349(w)	Deformation modes
	316(w)	310(w,br)	302(w)	Deformation modes
	269(m)		268(mw)	Deformation modes
	221(w)		231(w)	Deformation modes
	200(w,br)		189(w)	Deformation modes

[a] ν = stretching mode. [b] Intensities are given in parenthesis; *w* = weak, mw = medium weak, *m* = medium, *s* = strong, *vs.* = very strong, sh = shoulder.

The significance of the vibrational spectra is that they demonstrate that the products of reactions between MF_3 (M = In, Tl) and SbF_5 in aHF, used to record the Raman spectra, could be better formulated as $MF_3{\cdot}3SbF_5$ than purely ionic $M(SbF_6)_3$ compounds.

Crystal structure of solid SbF_5 consists of tetramers built from four SbF_6 octahedra sharing joint vertices.[24] SbF_6 units are linked by *cis*-bridging fluorine atoms. Vibrational spectra of liquid SbF_5 argues in favour of a *cis*-fluorine-bridged polymer.[25] Because of that, the great similarity between vibrational spectra of $InF_3{\cdot}3SbF_5$ and liquid SbF_5 is not surprising (Table 1, Fig. 11). In both cases we have strongly deformed SbF_6 units with two strongly elongated Sb–F_b bonds with F_b in *cis*-position and four much shorter Sb–F_t bonds. The bands in the 665–742 cm^{-1} region are assigned to stretching modes (Sb–F_t) between Sb atom and terminal fluorine atoms, meanwhile bands in the 450–533 cm^{-1} range are typical for Sb–F_b–M (M = metal atom) bridging.[26] Bands below 350 cm^{-1} were assigned to bending deformations.

Table 2 Vibrational data of $TlF_3{\cdot}3SbF_5$

$TlF_3{\cdot}3SbF_5$	
IR[a]	R
733(sh)	727(20)
721(s)	
712(sh)	714(90)
704(vs)	702(100)
670(sh)	662(sh)
	639(50)
626(m)	
591(sh)	
	537(5)
495(vs)	491(3)
478(vs)	
	455(5)
	392(7)
376(m)	
	357(5)
	309(5)
	256(70)
	202(10)

[a] Intensities are given in parenthesis; *m* = medium, *s* = strong, *vs.* = very strong, sh = shoulder.

Raman spectra of $TlF_3{\cdot}3SbF_5$ (Fig. 12, Table 2) were taken on powdered samples obtained by syntheses (eqn (1)) and also on selected single crystals. They were found to be identical. Vibrational spectra of $TlF_3{\cdot}3SbF_5$ together with Raman spectrum of $TlSbF_6$ are shown in Fig. 12, and frequencies given in Table 2. As a consequence of the lowering of the symmetry of SbF_6 unit in the solid state (site symmetry and correlation effects) and the strong cation–anion interactions in the crystal lattice, some vibrations which are otherwise Raman or infrared inactive in O_h symmetry, becomes active, and additionally, splitting of some vibrations may also occurs. Since $TlF_3{\cdot}3SbF_5$ gave very complex vibrational spectra no detailed assignment has been done. Similar as in the case of $InF_3{\cdot}3SbF_5$, a strong doublet at 478/495 cm^{-1} was observed in infrared spectrum of $TlF_3{\cdot}3SbF_5$. Its intensity and position are typical for compounds where strong interactions between two metal centers are present (M–F_b–Sb bridges).

The Raman intensity of an XY_6 octahedra (molecule or anion) normally follows the order $I(\nu_1) > I(\nu_2) > I(\nu_5)$, where ν_1, ν_2 and ν_5 belong to symmetric stretching, asymmetric stretching and bending of XY_6 group, respectively. Typical example represents Raman spectrum of $TlSbF_6$ (Fig. 12) with the most intensive band at 647 cm^{-1} (ν_1), two weaker bands at 275/287 cm^{-1} (ν_5) and one weak band 566 cm^{-1} (ν_2). In the Raman spectrum of $TlF_3{\cdot}3SbF_5$ the most intensive band is observed at much higher value ($\sim$708 cm^{-1}). Additionally, it is split into two bands (702 and 714 cm^{-1}) and for both of them the corresponding bands (704 and 721 cm^{-1}) could be found in the infrared spectrum of $TlF_3{\cdot}3SbF_5$. We could not find any similar example in available literature. Similar case was with Raman spectrum of $TlF_3{\cdot}AsF_5$ (ESI, Figure S3†).

Conclusions

Experimental results of reactions between group 13 metal trifluorides (MF_3, M = Al, Ga, In, Tl) and strong Lewis acids (SbF_5, AsF_5) in anhydrous HF as a solvent confirmed in

Table 3 Mass balances and chemical analyses of $InF_3{\cdot}3SbF_5$, $TlF_3{\cdot}3SbF_5$, and $TlF_3{\cdot}AsF_5$

	Mass balance		Chemical analyses					
	Calculated	Obtained	Calculated			Obtained		
Product	/g	/g	%In/Tl	%Sb/As	%F	%In/Tl	%Sb/As	%F
$InF_3{\cdot}3SbF_5$	0.600	0.632	13.97	44.43	41.60	12.0	44.0	40.6
$TlF_3{\cdot}3SbF_5$	0.866	0.9284	22.42	40.07	37.52	22.2	/	37.4
$TlF_3{\cdot}AsF_5$	0.647	0.647	47.39	17.37	35.24	48.3 ± 0.8	18.1 ± 0.3	34.6

literature expressed expectations[29] that preparation of cationic species by fluoride ion abstraction from MF_3 (M = Al, Ga, In, Tl) is highly unlikely. Nonreactivity of AlF_3 and GaF_3 is a consequence of their higher lattice energies in comparison to InF_3 and TlF_3. The isolated solids could be better formulated as fluorine-bridged polymeric adducts, *i.e.* $MF_3{\cdot}3SbF_5$ (M = In, Tl) and $TlF_3{\cdot}AsF_5$, than ionic $M(SbF_6)_3$ and $TlF_2(AsF_6)$ compounds. Extremely elongated Sb–F_b(–In) bonds observed in the crystal structure of $InF_3{\cdot}3SbF_5$, shows very high Lewis acidity of In^{3+}, meanwhile the acidity of Tl^{3+} is lower.

In the case of weaker Lewis acid, AsF_5, reaction proceeded only with TlF_3. It seems that only in this case, the fluoride ion affinity of AsF_5 is capable to overcome the unfavourable difference in the lattice energies between the reactants (*i.e.* TlF_3) and the products (*i.e.* $TlF_3{\cdot}AsF_5$), where the lattice energy of the former should be much higher then the lattice energy of the latter. The intermediate compound $TlF_3{\cdot}AsF_5{\cdot}2HF$ is a metastable phase.

Experimental

Caution

Anhydrous HF and some fluorides are highly toxic and must be handled using appropriate apparatus and protective gear.

Apparatus and reagents. Volatile materials (SbF_5, AsF_5, aHF) were handled in an all-Teflon vacuum line equipped with Teflon valves. The manipulation of the non-volatile materials was done in a dry box (M. Braun). The residual water in the atmosphere within the dry box never exceeded 2 ppm. The reactions were carried out in FEP (tetrafluoroethylene-hexafluoropropylene) reaction vessels (length 250–300 mm, i.d. 15.5 mm, o.d. 18.75 mm) equipped with Teflon valves and Teflon coated stirring bars. Prior to use, all reaction vessels were passivated with elemental fluorine. Fluorine was used as supplied (Solvay). Anhydrous HF (Fluka, Purum) was treated with K_2NiF_6 (Ozark Mahoning) for several hours prior to use. AlF_3 (Aldrich, 99.95%), GaF_3 (Aldrich, 99.99%) and InF_3 (Aldrich, 99.9%) were used as supplied. Since commercial "TlF_3" was yellow, it was treated by 20 bar of elemental fluorine at 473 K for three days in a 100 ml nickel reaction vessel. Resulted TlF_3 was colorless. Compounds SbF_5 and AsF_5 were synthesized by pressure fluorination of SbF_3 (Alfa Aesar, 99%) or As_2O_3 (Fluka, 99.5%), respectively, with elemental fluorine in a nickel reactor at 573 K.[30]

Techniques. Infrared spectra were taken on a Perkin-Elmer FTIR 1710 spectrometer on powdered samples between AgCl windows in a leak tight brass-cell. Raman spectra were recorded on Renishaw Raman Imaging Microscope System 1000, with He–Ne laser with wavelength 632.8 nm.

Reactions between MF_3 (M = Al, Ga, In, Tl) and AsF_5/SbF_5 in aHF. All experiments between MF_3 and SbF_5/AsF_5 were made in a similar manner, so only preparation of $InF_3{\cdot}3SbF_5$ is described. In a dry-box 0.73 mmol (0.125 g) of InF_3 was loaded into FEP reaction vessel. Then aHF (1.5 ml) was condensed onto InF_3 and excess of SbF_5 (1.40 g, 6.46 mmol) was added, both at 77 K. After warming of reaction mixture to the room temperature the solid phase completely dissolved and clear colourless solution was obtained in few hours. The solution was left stirring for 24 h and volatiles aHF and SbF_5 were pumped away.

There was no reaction observed in the MF_3 (M = Al, Ga)/SbF_5/aHF and MF_3 (M = Al, Ga, In)/AsF_5/aHF systems. Mass balances and chemical analysis of isolated $InF_3{\cdot}3SbF_5$, $TlF_3{\cdot}3SbF_5$, and $TlF_3{\cdot}AsF_5$ are given in Table 3.

Crystal growth of $InF_3{\cdot}3SbF_5$, $TlF_3{\cdot}3SbF_5$ and $TlF_3{\cdot}AsF_5{\cdot}2HF$. Single crystals preparation of $InF_3{\cdot}3SbF_5$ was carried out in a T-shaped apparatus made of two FEP tubes (19 mm o.d., and 6 mm o.d.). About 0.35 g of $InF_3{\cdot}3SbF_5$ was dissolved in ~2 ml aHF at 273 K. Clear solution was poured into the narrower tube. The evaporation of solvent from this solution was carried out by maintaining temperature gradient of about 10 K between wider and narrower tube of the apparatus for one month. Colourless single crystals of $InF_3{\cdot}3SbF_5$ formed.

In the case of $TlF_3{\cdot}3SbF_5$, 100 mg of the sample was dissolved in 2 ml of aHF, and clear solution was decanted into the narrower tube. The latter was kept at 273 K, meanwhile the wider one was cooled down, First to 257 K for 2 weeks, then to 232 K for additional 5 days. Colourless single crystals of $TlF_3{\cdot}3SbF_5$ formed.

TlF_3 was dissolved in 2 ml of aHF acidified with 1.0 g of AsF_5. Clear solution was poured into the narrower tube. The evaporation of the solvent from these solutions was carried out by maintaining a temperature gradient corresponding to about less then 10 K between both tubes for 8 months. The result of this treatment was to slowly condense the aHF from the narrower into the wider tube, leaving behind the crystals. Attempts to speed the crystallization (for example, higher temperature gradient) resulted in immediate precipitation of powdered non-crystalline product. Grown crystals of $TlF_3{\cdot}AsF_5{\cdot}2HF$ were isolated at 273 K.

Crystallization products were immersed in a perfluorinated oil (ABCR, FO5960, melting point 263 K) in a dry-box. Single crystals were then selected from the crystallization products under the microscope (at temperatures from 265 to 273 K)

Table 4 Summary of crystal data and refinement results for $InF_3{\cdot}3SbF_5$, $TlF_3{\cdot}3SbF_5$ and $TlF_3{\cdot}AsF_5{\cdot}2HF$

	$InF_3{\cdot}3SbF_5$	$TlF_3{\cdot}3SbF_5$	$TlF_3{\cdot}AsF_5{\cdot}2HF$
Crystal system	Trigonal	Trigonal	Monoclinic
Space group	$P\bar{3}c1$	$P\bar{3}$	P_21/c
a/pm	871.90(6)	940.8(16)	555.33(4)
b/pm	871.90(6)	940.8(16)	576.52(5)
c/pm	952.19(9)	859.7(14)	2192.87(19)
β (°)	/	/	93.279(4)
V (nm^3)	0.62688(9)	0.6590(19)	0.70092(10)
Z	2	2	4
M/g mol^{-1}	822.07	911.62	471.31
ρ_c/g cm^{-3}	4.355	4.594	4.466
T/K	200	200	200
μ/mm^{-1}	8.428	18.480	27.87
$R_1{}^a$	0.0398	0.407	0.0593
w$R_2{}^b$	0.0913	0.0972	0.1177
GOF^c	1.269	1.137	1.216

^{a} $R_1 = \Sigma||F_o| - |F_c||/\Sigma|F_o|$ for $I > 2\sigma(I)$. ^{b} $wR_2 = [\Sigma(w(F_o^2 - F_c^2)^2/\Sigma(w(F_o^2)^2]^{1/2}$ for $I > 2\sigma(I)$. ^{c} GOF $= [\Sigma w(F_o^2 - F_c^2)^2)/N_o - N_p)]^{1/2}$, where N_o = no. of reflns and N_p = no. of refined parameters.

outside the dry-box and then transferred into the cold nitrogen stream of the diffractometer.

Crystal structure determination

Single-crystal data were collected on Rigaku AFC7 diffractometer with Mercury CCD area detector using graphite monochromated Mo-Kα radiation at 200 K. The data were corrected for Lorentz and polarization effects. A multi-scan absorption correction was applied to all data sets. All structures were solved by direct methods using SIR-92[31] program and refined with SHELXL-97[32] software, implemented in program package WinGX.[33] In the structure of $TlF_3{\cdot}AsF_5{\cdot}2HF$ positions of hydrogen atoms were determined geometrically. The structure drawings were generated by Balls & Sticks, freely available software.[34] The crystallographic data and the details of the structure refinement are given in Table 4. Further details of the crystal-structure investigation may be obtained from the Fachinformationszentrum Karlsruhe, D-76344 Eggenstein-Leopoldshafen, Germany, on quoting the depository numbers CSD-421923 ($InF_3{\cdot}3SbF_5$), CSD-421924 ($TlF_3{\cdot}3SbF_5$) and CSD-421925 ($TlF_3{\cdot}AsF_5{\cdot}2HF$).

Acknowledgements

The authors gratefully acknowledge the Slovenian Research Agency (ARRS) for financial support of the present study within the research program: P1-0045 Inorganic Chemistry and Technology.

References

1 G. A. Olah, G. K. Surya Prakash, Á. Molnár and J. Sommer, *Superacid Chemistry*, John Wiley & Sons, Hoboken, 2nd edn, 2009, pp. 23–27.
2 K. O. Christe, D. A. Dixon, D. McLemore, W. W. Wilson, J. A. Sheehy and J. A. Boatz, *J. Fluorine Chem.*, 2000, **101**, 151.
3 R. Craciun, D. Picone, R. T. Long, S. Li and D. A. Dixon, *Inorg. Chem.*, 2010, **49**, 1056.
4 M. Broschag, T. M. Klapötke and I. C. Tornieporth-Oetting, *Chem. Commun.*, 1992, 389.
5 H. D. B. Jenkins, I. Krossing, J. Passmore and I. Raabe, *J. Fluorine Chem.*, 2004, **125**, 1585.
6 S. Rüdiger, U. Groß and E. Kemnitz, *J. Fluorine Chem.*, 2007, **128**, 353.
7 C. H. Barclay, H. Bozorgzadeh, E. Kemnitz, M. Nickkho-Amiry, D. E. M. Ross, T. Skapin, J. Thomson, G. Webb and J. M. Winfield, *J. Chem. Soc., Dalton Trans.*, 2002, 40.
8 E. Kemnitz, U. Groß, S. Rüdiger and C. S. Shekar, *Angew. Chem., Int. Ed.*, 2003, **42**, 4251.
9 T. Skapin, G. Tavčar, A. Benčan and Z. Mazej, *J. Fluorine Chem.*, 2009, **130**, 1086.
10 *Handbook of Chemistry and Physics*, ed. D. R. Lide, CRC Press, Boca Raton, 2003, 84th edn, pp. 12–25.
11 R. Hoppe and D. Kissel, *J. Fluorine Chem.*, 1984, **24**, 327.
12 I.-C. Hwang and K. Seppelt, *Z. Anorg. Allg. Chem.*, 2002, **628**, 765.
13 H. Shorafa and K. Seppelt, *Z. Anorg. Allg. Chem.*, 2009, **635**, 112.
14 W. Sawodny and K. Rediess, *Z. Anorg. Allg. Chem.*, 1980, **469**, 81.
15 J. Fawcett, J. H. Holloway and D. R. Russell, *J. Chem. Soc., Dalton Trans.*, 1981, 1212.
16 N. LeBlond, D. A. Dixon and G. J. Schrobilgen, *Inorg. Chem.*, 2000, **39**, 2473.
17 I.-C. Hwang and K. Seppelt, *Angew. Chem., Int. Ed.*, 2001, **40**, 3690.
18 Ch. Hebecker, *Z. Anorg. Allg. Chem.*, 1972, **393**, 223.
19 Z. Mazej, P. Benkič, A. Tressaud and B. Žemva, *Eur. J. Inorg. Chem.*, 2004, 1827.
20 Ch. Hebecker, *Z. Naturforsch B*, 1975, **30**, 305.
21 K. O. Christe, C. J. Schack and R. D. Wilson, *Inorg. Chem.*, 1975, **14**, 2224.
22 K. O. Christe, P. Charpin, E. Soulie, R. Bougon, J. Fawcett and D. R. Russell, *Inorg. Chem.*, 1984, **23**, 3756.
23 J. L. Forquet, B. Boulard and F. Plet, *J. Solid State Chem.*, 1989, **81**, 35.
24 A. J. Edwards and P. Taylor, *J. Chem. Soc. D*, 1971, 1376.
25 I. R. Beattie, K. M. S. Livingston, G. A. Ozin and D. J. Reynolds, *J. Chem. Soc. A*, 1969, 958.
26 Z. Mazej, *J. Fluorine Chem.*, 2004, **125**, 1723.
27 G. S. H. Chen, J. Passmore, P. Taylor, T. K. Whidden and P. S. White, *J. Chem. Soc., Dalton Trans.*, 1985, 9.
28 Z. Mazej, *Eur. J. Inorg. Chem.*, 2005, 3983.
29 R. Mews, E. Lork, P. G. Watson and B. Gortler, *Coord. Chem. Rev.*, 2000, **197**, 277.
30 Z. Mazej and B. Žemva, *J. Fluorine Chem.*, 2005, **126**, 1432.
31 A. Altomare, M. Cascarano, M. C. Giacovazzo and A. Guagliardi, *J. Appl. Crystallogr.*, 1993, **26**, 343.
32 G. M. Scheldrick, *SHELXL-97*, University of Göttingen, Germany, 1997.
33 WinGX (Farrugia, L. J., 1999).
34 T. C. Ozawa and Sung J. Kang, "Balls & Sticks: Easy-to-Use Structure Visualization and Animation Creating Program", *J. Appl. Crystallogr.*, 2004, **37**, 679, http://www.softbug.com/toycrate/bs/.

